JVI Accepts, published online ahead of print on 10 September 2014
J. Virol. doi:10.1128/JVI.01636-14

Title:

Accumulation of human-adapting mutations during circulation of A(H1N1)pdm09 influenza in humans in the UK

Running title: Human adaptation of A(H1N1)pdm09 during pandemic waves

Authors:

Ruth A. Elderfield[1], Simon J. Watson[5], Alexandra Godlee[2], Walt E.Adamson[6], Catherine I. Thompson[4], Jake Dunning[3] , Mirian Fernandez-Alonso[1], Deena Blumenkrantz[1], Tracy Hussell [2], The MOSAIC investigators, Maria Zambon[4], Peter Openshaw[3], Paul Kellam[5] and Wendy S. Barclay[1,*].

Addresses:

Sections of Virology[1] Leucocyte Biology[2] and Respiratory Medicine[3], Faculty of Medicine, Imperial College London, Norfolk Place, W2 1PG London, UK; Virus Reference Department, Public Health England, 61 Colindale Avenue, London, NW9 5HT, UK[4]; Wellcome Trust Sanger Institute, Wellcome Trust Genome Campus, Hinxton CB10 1SA, UK[5]; West of Scotland Specialist Virology Centre, Gartnavel General Hospital, Great Western Road, Glasgow G12 0YN, UK[6].

*Corresponding author
Email w.barclay@imperial.ac.uk, telephone +44 2075945035

Abstract

The influenza pandemic that emerged in 2009 provided an unprecedented opportunity to study adaptation of a virus recently acquired from an animal source during human transmission. In the UK, the novel virus spread in three temporally distinct waves between 2009 and 2011. Phylogenetic analysis of complete viral genomes showed that mutations accumulated over time. Second and third wave viruses replicated more rapidly in human airway epithelial (HAE) cells than first wave virus. In infected mice, weight loss varied between viral isolates from the same wave but showed no distinct pattern with wave, and did not correlate with viral load in the mouse lungs or severity of disease in the human donor. However, second and third wave viruses induced less interferon-α in the infected mouse lungs. NS1 protein, an interferon antagonist, had accumulated several mutations in second and third wave viruses. Recombinant viruses with third wave NS gene induced less interferon in human cells but this alone was did not account for increased virus fitness in HAE cells. Mutations in HA and NA genes in third wave viruses caused increased binding to α-2,6 sialic acid, and enhanced infectivity in human mucus. A recombinant virus with these two segments replicated more efficiently in HAE cells. A mutation in PA (N321K) enhanced polymerase activity of third wave viruses and also provided a replicative advantage in HAE cells. Therefore, multiple mutations allowed incremental changes in viral fitness which together may have contributed to the apparent increase in severity of A(H1N1)pdm09 influenza during successive waves.

Importance

Although most people infected with the 2009 pandemic influenza virus had mild or unapparent symptoms, some suffered severe and devastating disease. The reasons for this variability were unknown but the numbers of severe cases increased during successive waves of human infection in the UK. To determine the causes of this variation, we studied genetic changes in virus isolates from individual hospitalized patients. There were no consistent differences between these viruses and those circulating in the community, but we found multiple evolutionary changes that in combination over time increased the virus's ability to infect human cells. These adaptations may explain the remarkable ability of A(H1N1)pdm09 virus to continue to circulate despite widespread immunity, and the apparent increase in severity of influenza over successive waves of infection.

Introduction

In 2009 a novel H1N1 influenza virus (A(H1N1)pdm09) crossed the species barrier from swine into humans causing the first influenza pandemic of the 21st century. The swine-origin virus displayed a complex genotype including antigen gene segments derived from swine-adapted influenza viruses that had previously circulated on different continents, and an internal gene cassette known as the triple reassortant genotype (TRIG) first described in pigs in the late 1990s (1–3). The TRIG cassette contained two polymerase components, PB2 and PA, from an avian virus and the other, PB1, from a human-adapted virus. The NP, HA and NS gene segments of the pandemic H1N1 2009 virus were acquired from the classical swine virus lineage that has circulated in pigs since 1918 and had been maintained in North American swine viruses (4, 5). Classical swine influenza viruses shared an origin with the human H1N1 seasonal influenza viruses but the two had since undergone species-specific mutations in their respective hosts. The genetic distance between the HA genes was sufficient to cause a pandemic, despite the circulation of seasonal H1 viruses in humans from 1977 until 2009. The A(H1N1)pdm09 NP gene had adaptations associated with evasion of MxA from swine or humans (6). Finally, RNA segment 8 encoding NS1 and NEP proteins had accumulated many mutations that differentiated it from the NS segment of human-adapted influenza viruses. Notably the swine virus NS1 protein had become truncated through a termination codon at amino acid 220 in comparison to the human-adapted NS1 protein, which retained a typical NS1 length of 230 residues (5). A functional difference in the swine-origin NS1 was reported by Hale *et al.* (7) and confirmed by us (8) whereby the ability to bind to the human host cell factor CPSF 30 and limit host gene expression had been lost by the accumulation of at least 3 mutations in the C-terminal domain of the NS1

gene. Thus the virus that crossed from pigs to humans and sparked the 2009 pandemic was not optimized for human replication and transmission because its gene segments were swine-adapted.

In the United Kingdom, there were two waves of A(H1N1)pdm09 activity during the 2009-10 pandemic period: an initial out-of-season outbreak that started in April 2009 and peaked in July 2009, followed by a second wave in the autumn and winter of 2009-2010. In the first post-pandemic winter (2010-11), a third wave of A(H1N1)pdm09 activity was seen. This third wave was associated with an increase in infection and severity, and a shift in age demographics from children (0-15 years) and younger adults (16 to 44 years) to predominantly adults (9–12). Compared with the first two pandemic waves, the third wave was associated with more hospital admissions (8797 vs 7879 people), more people admitted to critical care (2200 vs 1700 people) and a greater number of deaths (474 vs 361 people) in England (13). Although there had been evidence of sequence variation in viruses in the second pandemic wave in the UK and elsewhere (14, 15), surveillance and antigenicity studies had reported no change in the antigenicity of the surface glycoproteins haemagglutinin (HA) and neuraminidase (NA), so a vaccine update was not warranted (14). Moreover, any change in antigenicity is unlikely to explain the increased severity of third wave viruses in the unvaccinated or those who had not previously contracted the virus. Nonetheless, it is possible that other genetic changes distinct from those with an antigenic effect may have led to increased circulation of the virus or enhanced virulence that accounted for the apparent increased severity in the UK's third wave. Indeed, Dorigatti and Ferguson recently modelled the UK third wave and concluded that the observed increased numbers of cases were most likely accounted for by an increase in virus transmission with a

commensurate increase in the numbers of severely ill. They suggested this could be due to weather conditions that winter being particularly cold and dry and favouring virus transmission events, or to a change in the inherent transmissibility of the virus itself, or both (16). Here we report genetic variability across the three waves of influenza A(H1N1)pdm09 in the UK and identify non-synonymous variants that define the third wave viruses. We show that mutations in HA and NA, the PA component of the polymerase complex and the NS1 interferon antagonist protein enhanced the virus' ability to replicate in human airway cells.

Materials and methods

Cells. Madin-Darby canine kidney (MDCK), Human embryonic kidney (293T), and Newborn pig tracheal (NPTr), cells were grown in Dulbecco's Modified Eagle Medium (DMEM) supplemented with 10% Foetal calf serum (FCS). Mucil-Air™ cultures of human nasal epithelium (HAE) (Epithelix) were grown in Mucil-Air media. All cells were maintained at 37°C in 5% CO_2.

Patient recruitment and sampling. MOSAIC recruited adult and paediatric patients admitted to hospital with suspected influenza virus infection in London and Liverpool between December 2009 and February 2011. Infection with seasonal influenza A H3N2, influenza B or A(H1N1)pdm09 viruses was confirmed locally by viral PCR according to regional protocols. Patients were approached for recruitment and initial (T1) sampling as soon as possible following admission to a MOSAIC-associated hospital. Nasopharyngeal aspirate and viral throat swab samples were obtained according to the study SOP. Patients with comorbidities were not excluded. Different severities of illness were included and severity was graded as follows: grade 1 = no respiratory compromise (oxygen saturation >93% on room air); grade 2 = respiratory compromise requiring non-invasive oxygen supplementation; grade 3 = respiratory compromise requiring invasive mechanical ventilation and oxygen supplementation. The MOSAIC study was approved by the NHS National Research Ethics Service, Outer West London REC (09/H0709/52, 09/MRE00/67).

Viruses. Influenza viruses were isolated from clinical specimens by the Respiratory Virus Unit, Public Health England, Colindale, London. Briefly, clinical specimens including nasopharyngeal aspirate (NPA), viral throat swab in virus transport media (VTM), bronchial alveolar lavage (BAL) or endotracheal aspirate (ETA) were

transported to PHE frozen on dry ice. For virus isolation 200µl clinical specimen was inoculated onto monolayers of Madin-Darby Canine Kidney (MDCK) cells or the SIAT-1 cell derivative in virus isolation tubes and allowed to adsorb for one hour (17)Cells were incubated in serum-free Earles MEM in the presence of 1.25 µg/ml TPCK-treated trypsin (Worthington) on a rolling drum at 33°C for a maximum of seven days with regular observation for viral cytopathic effect (CPE). Blind passage on fresh cells for a further 7 days was performed where necessary. Virus growth was determined by haemagglutination assay using turkey or guinea pig red blood cells. One further virus passage was made to generate a large stock of virus for distribution to the MOSAIC consortium.

Plasmid based reverse genetics. The reverse genetics viruses were generated as previously described (8) from plasmids either synthesised (GeneArt) from A/England/195/2009 whole genome sequence and A/England/687/2010 segment 4 sequence, or generated by site-directed mutagenesis (Stratagene Lightening mutagenesis kit) of A/England/195/2009 plasmid sequence with point mutations necessary to create A/England/687/2010 amino acid sequence. The plasmids were sequenced to confirm presence of required mutations and absence of unwanted variations. Primer sequences available upon request. Reverse genetics viruses were generated using the 12 plasmid system with either A/England/195/2009 or A/England/687/2010 polymerase I clones and helper polymerase of A/Victoria/3/75.

Virus replication in cell lines and primary airway cultures. Confluent cell monolayers were infected with equal PFU of each virus at an MOI of 0.01 or 0.001 as specified in the main text. The cells were incubated in the inoculum for 1 hour then the inoculum was removed, cells washed with PBS and overlaid with DMEM supplemented with NEAA, Penicillin/Streptomycin and TPCK treated trypsin and incubated at 34□C in

166 5% CO2. Growth was assessed by well sampling at fixed timepoints and titrated on
167 MDCK cells by plaque assay. For infection of Mucil-Air cultures™, the apical surface
168 (air interface) was washed with serum free media prior to infection, then washed
169 again after the inoculation. Viral titre was assessed by sampling from the apical
170 surface by the addition of 200 µl of serum free media, incubation for 15 minutes and
171 removal of the media. The basal layer was sampled for cytokine analysis, with an
172 equal volume of Mucil-Air media replacing that removed.

173 *Virus competition assays*. Mucil-Air™ cells were washed with serum free DMEM
174 prior to inoculation with a 50:50 mix of two viruses at a total MOI of 0.001. The cells
175 were incubated for one hour prior to removal of the inoculum and washing with SF
176 media. The apical layer was sampled every 12 hours as above. Viral RNA was
177 extracted from the supernatant with a Qiagen Qiamp vRNA kit and processed for
178 Ilumina deep sequencing. Each assay was run in triplicate.

179 *Minigenome polymerase assays*. The coding sequence for the PB1, PB2, PA, and
180 NP proteins was amplified using KOD polymerase (Novagen) and primers containing
181 restriction sites to allow incorporation into pCAGGs expression vectors. To introduce
182 alternative amino acids into the coding sequence, site-directed mutagenesis was
183 undertaken on the reverse genetic genomic plasmids. Primers are available on
184 request. pCAGGs expression plasmids for PB1, PB2, PA and NP proteins were
185 transfected onto a confluent layer of 293T cells using Lipofectamine 2000 and
186 Optimem in the concentration ratio of 1:1:0.5:2 respectively, . Additionally a plasmid
187 encoding a minigenome firefly luciferase reporter flanked by the promoter region of
188 the influenza virus' segment 8 and either a Renilla or β-galactosidase transfection
189 control plasmid were co-transfected with the mini-genome complement. Cells were

incubated with the transfection mix for 24 hrs at 34□C at 5% CO2. Then supernatant was removed, the cells washed and 100 ul of passive lysis buffer added (Promega). The cells were freeze thawed and lysates analysed with the dual luciferase reporter system (Promega) on the FLUOstar OMEGA (BMG labtec). All assays were run in triplicate, with each assay being repeated a minimum of 3 times.

Interferon reporter assays. A plasmid with the interferon β–promoter region upstream of a firefly luciferase reporter was transfected along with a β-galactosidase or Renilla control plasmid into 293T cells in suspension using Lipofectamine 2000 and Optimem. 293T cells were adhered to plates pre-treated with Poly-L-Lysine and incubated overnight. The cells were then infected with virus at an MOI of 3, incubated at 37□C for one hour prior to inoculum removal, washing and overlaying with DMEM with 10% FCS. The cells were then harvested at set time points by the removal of media, washing with PBS and the addition of passive lysis buffer and passed through a freeze thaw cycle, prior to detection with the dual luciferase reporter system (Promega) on the FLUOstar OMEGA (BMG labtec). All assays were run in triplicate, with each assay being repeated a minimum of 3 times.

Mouse experiments. All animal procedures and care conformed strictly to the United Kingdom Home Office Guidelines under the Animals (Scientific Procedures) Act 1986 and the protocols were approved by the Home Office of Great Britain (License number: 70/6646).

Fifteen weight matched female Balb/C mice anesthetized with isoflurane were inoculated with 7.5 $x10^5$ or $2x10^5$ PFU of each influenza virus. Mice were weighed daily and any mice falling below a 30% weight loss threshold were sacrificed. At day 2 and day 4 post infection, 5 mice from each experimental group were sacrificed and

the lungs harvested. Whole lungs were weighed and homogenised in the presence of 1 ML of PBS and split into aliquots. An aliquot of lung homogenate from each mouse was subjected to titration by plaque assay. Results are expressed in ML of the homogenate as whole mouse lungs were homogenised in a standardised volume of PBS.

Interferon detection. Aliquots of mouse lung homogenate were tested for the presence of mouse interferon using the Verikine interferon α kit (R&D Systems) according to the manufacturer's instructions and then measured on the FLUOstar OMEGA (BMG labtec). Each sample was run in duplicate.

Phylogenetic analysis. Complete genomes of samples sequenced by the MOSAIC Consortium were aligned against all complete A/H1N1/09 genomes up to 2011 present in NCBI's Influenza Virus Resource database (18). To improve tree readability, this set of 2084 genomes was down-sampled using custom Python scripts, ensuring that the topology of the phylogenetic tree was maintained. Phylogenetic trees were inferred using a neighbour-joining clustering method with branch lengths and substitution parameters estimated using the Tamura-Nei model under the maximum composite likelihood method implemented in MEGA version 6.06 (19). Tree robustness was evaluated by boostrapping with 1000 pseudo-replicates.

Statistical analysis. All statistical analysis was conducted using GraphPad Prism software®. Virus replication, IP-10 and IFN cytokine production and the mucus inhibition assays were assessed by unpaired T-Tests compared to the A/195 first wave isolate. The interferon and minigenome assays were assessed by repeated

measures or ordinary one way anova with Tukey's multiple comparison test as appropriate.

Results

The Mechanisms of Severe Acute Influenza Consortium (MOSAIC) study was formed to investigate why some individuals infected by the pandemic H1N1 influenza virus developed severe symptoms requiring hospitalisation whilst others developed a milder coryzal illness. MOSAIC recruited 85 patients admitted to hospital with influenza-like illness in the winter of 2009/10 and a further 172 in winter 2010/11. Nasopharyngeal aspirate (NPA) and viral throat swab specimens were collected from patients for attempted isolation of virus strains by culture in MDCK cells, assessment of viral titre by qRT-PCR and whole genome sequencing directly from the clinical sample.

Evolution of influenza A(H1N1)pdm09viruses showed a distinct UK third wave lineage

Clinical samples, either NPA or throat swabs that were positive for influenza A(H1N1)pdm09 RNA were prepared without virus isolation or passage and sequenced by either the Roche Genome Sequence FLX 454 or Illumina Genome Analyzer IIx platforms as previously described (20), and assembled into full genomes as described (21). Background whole-genome pandemic sequences were downloaded from NCBI's Influenza Virus Resource database (18) and aligned against the UK first, second and third wave genomes. Phylogenetic analysis shows that viruses from the first two pandemic waves were closely related, consistent with the proposed persistence of the first wave lineages into wave two in the UK (20). However, viruses detected during the third wave (winter of 2010-2011) were genetically distinct, with the majority of genomes clustering in a separate monophyletic clade (Figure 1). Across the second and third waves in the UK, viruses

from hospitalised patients were phylogenetically indistinguishable from community and non-hospitalised control patients and did not contain shared genome variants that could confer an enhanced pathogenicity (Figure 1). We assessed amino acid changes fixed in the majority of viruses, identifying 21 common changes across all segments of which 12 were unique to third wave viruses (Table 1). These changes also accumulated in second and third wave virus isolates from other regions of the UK and from the rest of the world (Table 2), except for G189D in NS1. We also checked for nucleotide differences in segment 2 that would affect the translation of PB1-F2 and/or N40 open reading frames but found none.

Clinical isolates from the first, second and third pandemic wave varied in their growth kinetics in primary human airway cultures.

The lack of a common genetic difference between influenza viruses isolated from severe or mild influenza cases in each wave suggests that the observed increase in overall severity in the third wave may be related to a general property of wave three viruses, which should be reflected in virological differences between first, second and third wave viruses.

To assess virus differences we isolated virus from clinical samples in SIAT-MDCK cells for a subset of viruses selected in accordance with their placements on the phylogenetic tree in figure 1. We infected MDCK cells or primary human airway epithelial (HAE) cultures or mice with 9 different clinical isolates from the second wave (3 viruses) and the third wave (6 viruses), and compared growth and outcome of infection with the first wave prototypic UK A(H1N1)pdm09 virus, A/England/195/2009. Clinical data from patients from whom these isolates were obtained are shown in Table 3. We recorded the differences in viral RNA load in

NPA at time of recruitment (T1 NPA titre), the severity score for the patient and the presence of patient co-morbidities. With the caveat that the delay between symptom onset and recruitment varied from patient to patient (day since symptom onset), we did not find any correlation between viral load and severity score for this subset of the MOSAIC cohort.

In vitro, first, second, and third wave viruses used to infect MDCK cells did not show a consistent difference in replication pattern according to respective waves, although there was small variation between individual isolates (Figure 2A). In HAE cell cultures the pattern of virus replication was more diverse and correlated with respective waves. Although two viruses, one from the second (A/47) and one from the third wave (A/213), displayed similar growth kinetics to the prototypic A/195 virus, most second and third wave viruses displayed a growth advantage at 24 and 48 hours post-infection in human airway cells. Using a different HAE culture code (primary cells obtained from a different donor), a representative third wave clinical isolate, A/687, displayed a consistent 2 $\log_{10}$ growth advantage at the 24 and 48 hour time points, with a peak titre of 10^8 PFU/ml compared with 10^6 PFU/ml for the A/195 first wave virus at 48 hours post infection ($p=0.02$) before the virus titres became similar at 72 hours post infection (Figure 2c). Strikingly, in pig tracheal cell cultures (NPTr) the third wave virus A/687 was compromised in growth (Figure 2c). In other human lung cell lines such as Calu-3 the 1st wave virus also replicated more efficiently than the 3rd wave virus although the difference was not as pronounced as in the pig cell line. This suggests that the adaptation in 3rd wave virus might be conferred by features only present in the well differentiated complex HAE cultures.

Outcome of infection in the *in vivo* Balb/c mouse model did not correlate with patient severity or growth in human airway cultures.

313 In order to assess the *in vivo* characteristics of this panel of clinical isolates we
314 utilised a mouse model. Balb/c mice were infected intranasally with each of the panel
315 of viruses. After a dose of 2 x 10^5 PFU, the A/195 first wave isolate caused >20 %
316 weight loss by day 5 post infection (Figure 3a). Some of the second and third wave
317 viruses inoculated at the same dose were less pathogenic in mice as ascertained by
318 less weight loss, for example the A/687 third wave virus induced only 2% weight loss
319 and no mortality (Figures 3b & c). Mouse mortality (due to humane cull through
320 weight loss)was observed in all three of the sets of mice infected with the second
321 wave viruses, but only in two sets (A/689 and A/672) of the third wave infected mice.
322 Statistically, only the A/09 infected mice did not show a difference in weight loss to
323 the A/195 infected mice, the A/47 and the A/689 mice groups displayed a statistical
324 difference only on two and three days respectively. The differences in weight loss
325 and mortality in mice did not correlate with the severity scores assigned to the
326 human patients infected with the same virus (Figure 3a, b & c and Table 3).
327 Interestingly, the viral loads in the mouse lung at day 2 or 4 post infection did not
328 show the same pattern as titres in HAE culture infections, with a trend towards lower
329 virus lung titres at day 2 for the second and third wave viruses compared to A/195
330 (Figure 3d). For example, the first wave A/195 virus replicated to high levels in mice,
331 whereas the third wave A/687 virus replicated comparatively poorly, but in HAE cells
332 the situation was reversed (figure 2c). However in some cases the reciprocal pattern
333 between HAE replication and mouse pathogenicity was not maintained: A/672, which
334 had similar growth in HAE as A/687, replicated to a higher titre, induced high weight
335 loss of around 15 % and led to 20 % mouse mortality. There are only four coding
336 genetic differences between these two third wave viruses: HA L176I; NS1 I123V,
337 PB1 I12T and PB2 N556S.

The most obvious trait that associated with virus wave was a clear association between the interferon (IFN) α level in the mouse lung and the wave of isolation for each virus; levels of IFN in lungs of mice infected with second wave viruses were lower than for A/195, and the lowest IFN levels were in third wave virus infected mice lungs (Figure 3e). The lower IFN production as the waves progressed could reflect the virus adapting to better control the host immune system. The same patterns of weight loss, lung titres and lung interferon levels for each isolate were observed in a separate experiment where mice were infected with 7.5×10^5 PFU (data not shown).

Virus with segment 8 of the third wave virus induced less type I interferon.

The increased interferon in lungs of mice infected with first wave virus might be driven by higher viral loads. However viral loads in lung at day 2 were not always higher in mice infected by second wave than by third wave viruses, but IFN levels were higher (Figure 3d and e). We hypothesized that mutations in the virus between second and third wave may have enhanced the virus' ability to control the innate immune response. NS1 protein encoded on RNA segment 8 is the major interferon antagonist of influenza A virus. Sequence analysis showed third wave viruses possessed a cluster of amino acid changes in the NS1 protein, in various combinations at positions E55Q, P114T, I123V,and G189D (Table 1). A third wave isolate A/687 possessed three of these changes within the effector domain of the NS1 protein; 114T, 123V and 189D. The G189D variation also changed the coding sequence of the NEP protein (V32I) because the NS1 and NEP open reading frames overlap at this region. Under the conditions used for these assays IFNβ was undetectable in apical washes or in basal medium from infected HAE cultures. Therefore we assessed the virus' ability to counteract the production of an innate induced cytokine, IP-10. At 16 hours post infection with a high multiplicity of virus,

significantly less IP-10 was secreted from HAE cells infected with the A/687 virus compared to the first wave virus A/195 (Figure 4a). Levels of two other cytokines, IL-6 and IL-8 were also lower in basolateral media following infection of the HAE cells with 3rd wave virus (data not shown) but the difference did not reach significance. IFN was not detectable in samples collected form the HAE cells after infection with either virus.

To further assess the role of the NS gene mutations in controlling the cytokine response, we generated recombinant viruses with the segment 8 RNAs exchanged. The A/195 reverse genetics (RG) system described previously was generated by synthesizing the cDNAs for this strain *de novo* (8, 22). The A/687 reverse genetics virus was created by site-directed mutagenesis of the A/195 plasmids wherever an amino acid change was present, for seven of the gene segments. The gene segment encoding the A/687 HA was synthesised *de novo*.

293T cells transiently transfected with an IFNβ promoter luciferase reporter construct were infected with each of the 7:1 single gene reassortant viruses or with the isogenic A/195 or A/687 wild type reverse genetics (RG) viruses (Figure 4b) (23). The A/687 RG virus induced a significantly lower luciferase signal than A/195. The induction of the IFN β promoter was decreased relative to isogenic A/195 virus when the 687 NS gene was present, and significantly increased for the A/687 virus with A/195 NS..

Since there was also a difference in NEP coding between these two viruses we tested whether the NS1 itself had altered activity as an interferon antagonist when expressed exogenously. At 3 different doses of NS1 expression, the 3rd wave NS1

protein was significantly better able to control the expression of luciferase driven by an interferon promoter in NDV infected cells (Figure 4c).

The HA and NA genes of third wave viruses displayed different receptor binding preferences, enhanced infectivity in human mucus and conferred enhanced growth in HAE cell cultures over first wave viruses.

Second and third wave UK viruses displayed wave-associated amino acid changes in the HA and NA protein (Table 1). A collection of eleven MOSAIC virus isolates representative of the three waves and including A/195 (first wave), A/06 (second wave), and A/675 and A/687 (third wave) from the panel of nine viruses studied above, were tested in a haemagglutination assay using erythrocytes from different species (guinea pig, turkey and chicken), which are known to differ in the specificity and density of sialic acids expressed on their cell surface (24). All viruses displayed comparable binding to guinea pig and turkey erythrocytes, but the second and third wave isolates displayed lower binding to chicken red blood cells relative to A/195 (Figure 5a). The only exception was A/675, which has an M227I (230 in H3 numbering) amino acid variation near the receptor-binding pocket and retained strong binding to chicken erythrocytes. HA assays performed with RG A/195 and A/687 viruses recapitulated the general pattern seen for the panel of isolates; the relative binding of the first wave virus for chicken erythrocytes was higher than for the third wave virus (Figure 5b).

A/687 virus differs from A/195 by eight amino acids in the HA protein and four in the NA protein. To test if the changes in HA and NA alone were sufficient to confer the observed growth advantage in human airway cells (Figure 2b and c), we generated 6:2 recombinant viruses with the A/687 HA and NA combined with A/195 internal

proteins or the A/687 internal genes with the HA and NA of A/195, and compared their replication with that of isogenic wild type RG A/195, or RG A/687. The virus with the A/687 internal genes coupled with 1st wave HA and NA replicated to a lower titre than whole A/687 virus, and conversely the virus with A195 internal genes and 3rd wave HA and NA replicated to higher titres than whole A/195 virus. However the differences in replication did not reach statistical significance (Figure 5c). This suggests that both internal and external genes contribute to the enhanced replication of 3rd wave virus in HAE cultures but neither genes sets are sufficient to reproduce the phenotype alone.

To investigate a role for the third wave NA protein in enhanced replication in HAE cultures, we generated a 7:1 RG virus with 7 segments from the A/195 virus and RNA segment 6 which encodes the NA protein from A/687. This virus and the isogenic A/195 virus were then incubated in the presence of human respiratory mucus for 60 minutes prior to infection onto MDCK cells. The number of plaque-forming foci were counted and the percentage reduction in infectivity was calculated (25). The virus carrying the third wave NA gene segment displayed an increased ability ($p=0.044$) to overcome inhibition of infectivity by human mucus, which is an important factor in the ability of virus to infect and spread in the human airway (Figure 5d).

The mutation in PA, N321K of third wave viruses conferred enhanced replication in a minireplicon assay and in viral competition assays.

Mutations in other genes of the second and third wave viruses may have also contributed to human adaptation and enhanced replication in HAE. In the polymerase proteins and nucleoprotein of the A/687 virus there were seven amino

434 acid changes from A/195 polymerase genes, three of which were unique to the
435 majority of the third wave viruses in the UK. These three changes are at PB2
436 V344M, I354L and PA N321K (Table 1).

437 In order to assess whether these amino acid changes altered the activity of the viral
438 polymerase, we created two sets of expression plasmids that allowed reconstitution
439 of polymerase components from either A/195 or from A/687 virus. For the A/195
440 constellation we used a PA plasmid with the glycine 3 mutated to aspartic acid, since
441 this difference was atypical amongst first wave viruses (17). Each viral polymerase
442 was reconstituted in a minireplicon reporter assay in 293T cells as previously
443 described (26). The third wave A/687 polymerase and nucleoprotein complex
444 consistently directed higher amplification and expression of the luciferase signal from
445 the minireplicon in human cells than the A/195 polymerase constellation ($p=<0.001$)
446 (Figure 6a).

447 In order to discern if this enhancement of polymerase activity was a result of amino
448 acid changes in a single protein, the minireplicon assays were carried out with single
449 protein exchanges. A dramatic 10-fold decrease in signal was observed when the
450 A/195 PA protein was paired with the A/687 PB1, PB2 and NP proteins. The
451 reciprocal exchange saw the converse result, although the increase in polymerase
452 activity when A/687 PA was introduced into the A/195 polymerase constellation was
453 not statistically significant (Figure 6a).

454 To assess whether the PA N321K mutation led to an enhancement of replication in
455 the context of whole virus, we generated a 7:1 (PA) RG virus in which every genomic
456 segment except for the A/687 PA segment that was derived from A/195. Replication
457 competition experiments starting with a 50:50 mix in triplicate HAE cultures were

458 analysed by deep-sequencing using Illumina sequencing technology, and showed
459 the virus with the PA 321K from the third wave genotype rapidly dominated the viral
460 RNA population in all 3 biological replicates, ($p=0.0078$, <0.0001 and <0.0001 at 48,
461 72 and 96 hours respectively when assessed as a percentage of total reads in the
462 unpaired T test), illustrating a growth advantage in human cells conferred by this
463 amino acid change (Figure 6b).

464

Discussion

In the UK there was a reported increase in severity of the pandemic H1N1 virus as the waves of influenza infection progressed from its emergence in spring 2009 until end of winter 2011(10, 12). It has been suggested that this can be attributed to a shift in the behaviour of the infected population due to a change in public health responses (10, 13). However this explanation does not exclude host adaptations in the influenza virus itself that might also have contributed to the change in severity associated with A(H1N1)pdm09 infection. If the virus was responsible, there may have been a specific virulence factor that appeared in many or all of the hospitalised cases, however we find no evidence for this here. We can discern from whole-genome sequence data provided by FLUWatch, FF100, PHE, RCGP and the isolates derived from the hospitalised MOSAIC patients over three waves of infection in the UK, that the viruses derived from hospitalised patients did not vary genetically from those found within the community, consistent with Galliano *et al.* for the second wave (27).

Alternatively, a constellation of adaptive changes that accumulated in the virus as it circulated in the community could make it more likely that a higher proportion of individuals would become infected, with possibly more efficient early virus replication, leading to more severe infection in some people.

A great deal of effort worldwide has been put into tracing amino acid changes in the pandemic H1 HA, and to a lesser degree the NA (28–37). This emphasis on the glycoproteins is understandable due to their antigenic properties and importance in determining antiviral susceptibility. Indeed, various functional consequences of naturally occurring amino acid changes in the NA and HA proteins have already

been demonstrated using animal models (38–43). In our MOSAIC hospitalized cohort we did not detect specific HA mutations described by others to affect A(H1N1)pdm09 virulence, for example HA D222G, which purportedly facilitates better binding to α2,3 linked sialic acid-linked receptors in the lower respiratory tract (44–47), changes in glycosylation (48) or antigenicity (49) were not present. Other groups have suggested that HA D222G is relatively common is severe cases (44–47).The D222G mutation has been suggested to sometimes arise during virus culture as an artefact, and may also only be present as a minority variant in samples taken at certain times during the infection. We do not know why it was not detected in our MOSAIC cohort.

We detected a different type of phenotypic change associated with the HA protein of the third wave viruses compared to the first wave isolate. A comparison of the viruses' relative ability to haemagglutinate chicken, turkey, or guinea pig red blood cells indicated a relative increase in affinity to α-2-6 linked sialic acids and a concomitant decrease in the ability to bind to α-2-3 linked sialic acids for the majority of the third wave isolates. This alone may have increased the ability of the virus to infect the human upper respiratory tract, accounting for the greater replication of A/687 in HAE cells. That the lost affinity for the α2-3 sialic acids is observed in both second and third wave isolates would implicate one or more of the previously reported variations in the HA I32L, D97N, S185T, E374K and S451N (27). A recent publication by de Vries *et al.* (50) indicated a change in receptor binding caused by an S185T mutation. We also note the recent publication from Cotter *et al.* (51) showing that later isolates of A(H1N1)pdm09 virus contained pH-stabilising mutations in HA, which enhanced their replication in the ferret upper respiratory tract. This mutation at HA residue E374K (H1 numbering), is present in 5 of 6 third wave

514 viruses in our subset (Table 1) and may also have contributed to the increased
515 replication in HAE cultures we observed (Figure 2b).

516 There may also be a contribution of NA to the increased propagation of third wave
517 virus in HAE (Figure 5c). All of the second and third wave viruses in our cohort had
518 NA mutations V106I and N248D compared to first wave A/195. These are proposed
519 to enhance viral stability though modifications in pH tolerance in acidic conditions,
520 although we did not assess this phenotype (52). However, we did observe an
521 increase in the ability of virus with third wave NA to retain its infectivity in human
522 mucus, a property linked with efficient replication in HAE and transmission in ferrets
523 (23). Several other research groups have already investigated variation between
524 individual isolates of the A(H1N1)pdm09 lineage. These publications describe a few
525 selected isolates without considering their phylogenetic relationships, from mild,
526 severe or fatal cases, and characterize their sequences and phenotypes in various
527 animal models (41, 53–55). A correlation has sometimes been observed between
528 the outcome of infection in animal models and the severity of the human case from
529 which the isolate had been obtained; this was not the case in our study. Rather, we
530 find increased replication in primary human cells is often accompanied by decreased
531 virulence in the murine model. It is well recognized that the mouse is not a good
532 model host for human-adapted influenza viruses.

533 Our work suggests that changes to internal viral proteins, including NS1 and PA,
534 occurred during evolution of the third wave viruses and adapted them for increased
535 replication in human cells. Others have also recently suggested that mutations have
536 occurred in the virus polymerase since its transfer to humans that may enhance
537 replication or transmission (56, 57). These previously described mutations may
538 contribute to some of the enhanced polymerase activity we measured for the A/687

539 third wave virus polymerase, but our *in vitro* polymerase reporter system also
540 indicated that the N321K amino acid change in the PA protein, not previously
541 reported, drove enhancement of viral polymerase activity. How it may achieve this is
542 unclear. PA is known to interact with host factors such as transcriptional modulator of
543 RNA polymerase II (RNAPII) hCLE (58, 59) and the minichromosome maintenance
544 complex (60). The PA gene segment of A(H1N1)pdm09 virus was originally derived
545 from an avian source during the formation of the TRIG internal gene cassette.
546 Bussey *et al.* have already described three amino acids (85I, 186S and 336M)
547 present in the A(H1N1)pdm09 PA that are not usually present in PA of avian viruses.
548 They concluded that these three mutations together may have contributed to the
549 ability of this polymerase complex to function better in mammalian cells. The
550 mutation at residue 336 is situated close to amino acid 321 on the crystal structure
551 (61).

552 PA 321K was, until now, rare in swine adapted influenza viruses, occurring in only
553 1.85% of sequences of all influenza A subtypes, and 3% of swine H1N1 viruses
554 before the emergence of A(H1N1)pdm09 in 2009. It will be interesting to see if there
555 is an increase in the occurrence of a lysine at this position in swine as the
556 A(H1N1)pdm09 virus circulates in pigs or is reintroduced to this host through contact
557 with humans after the third wave. Only 2.06% avian isolates have PA 321K. This
558 amino acid does not occur in the PA segment of seasonal human influenza viruses
559 but the prevalence of the lysine variation in human isolates of pandemic H1N1
560 increased sharply as sequences from later in the pandemic were submitted to NCBI,
561 supporting its prevalence during and after the third wave. We expected the
562 advantage conferred by this single PA mutation engineered alone to be subtle and
563 therefore analysed the effect using a competition assay rather than by direct

564 comparison of growth curves. Previously we have shown that the NA mutation
565 H275Y in 1st wave virus conferred a replicative cost that was not detected by growth
566 curve analysis but only by competition assay (62)). Indeed we found that virus with
567 the single PA change 321K outgrew 321N virus in 3 biological replicates of HAE
568 cultures. This type of fitness assay could be useful in predicting the selection of
569 mutations that confer subtle advantage.

570 The other gene segment we investigated in detail here was that which encodes the
571 NS1 protein. Interestingly, we found a cluster of mutations in NS1 that slightly
572 enhanced its ability to control the innate immune response, including IFN and other
573 cytokines. In the murine model decreased virus titre in the lungs early in infection
574 with third wave viruses may also have contributed in part to a decreased IFN
575 production. However in human airway cultures where third wave virus replicated
576 robustly, we observed decreased IP-10 production in comparison with A/195. We
577 attribute this to changes in NS1 because other known antagonists of the interferon
578 response such as PB1-F2 were not different between these two viruses. Moreover, a
579 6:2 recombinant virus with HA and NA from 3rd wave on 1st wave internal gene
580 constellation induced higher IP-10 and other cytokine responses in HAE cells than
581 whole 1st wave virus (data not shown). This suggests that the differences in cytokine
582 response were not accounted for in this case by changes in receptor binding
583 specificity that affected ciliated vs nonciliated cell tropism in the HAE cultures as
584 suggested by Ramos et al. 2011(63)). One explanation for our findings is that the
585 NS1 protein had acquired some ability to bind to host cell factor CPSF30 and inhibit
586 host mRNA processing, a mechanism by which other human-adapted influenza
587 viruses have enhanced their control of the human innate immune response (64, 65).
588 Indeed, exogenous expression of the A/687 NS1 gene inhibited the expression of a

reporter gene from a polymerase II promoter significantly more efficiently than the NS1 gene from A/195 did (data not shown). This property is associated with an ability to bind and inhibit CPSF30 and may account for the difference we observed in heterologous control of induced interferon (Figure 4c). Hale *et al.* had already predicted some mutations in A/California/04/2009 virus by which this could be achieved, one of which is common to the A/687 NS1, G189D (7). That study also reported rather subtle effects on virus replication for viruses that were engineered to have CPSF30 binding. Notably one virus isolated in the third wave, A/689, which phylogentically lies closer to second wave viruses, was associated with higher cytokine levels than other third wave viruses in mouse lungs.

In conclusion, using a collection of A(H1N1)pdm09 viruses chosen based on phylogenetic divergence we have shown amino acid changes in HA, NA, NS1 and PA in later waves led to functional changes in individual viral genes that conferred increased replication in primary human airway cells, suggestive of human adaptation. The increase in viral fitness overall may facilitate increased transmission as suggested by Doriggati and Ferguson (2013) but the lack of virus genetic differences between severe and community influenza cases suggests these changes are not on their own sufficient to confer severe disease (16), especially as there is evidence of high levels of asymptomatic or unreported illness during the first three waves of A(H1N1)pdm09 virus activity in the UK (12). Infection of those predisposed to more severe disease may have been more likely in the third wave because of the differences in viral replication, host immune modulation and viral persistence in the host and the external environment (66–68).

Author contributions/ Acknowledgements:

Wrote the Manuscript: RE, SW, WB, PK, PO

Developed clinical protocols, helped collect clinical samples and clinical data, and contributed to manuscript revision: JD

Contributed viral isolates and sequencing data: SW, RE, WA, BC, CT, MZ; MOSAIC Consortium, Flu watch, FF100, RCGP.

Performed and/or planned experiments: RE, AG, WB, TH, PO, MFA, SW, PK, DB.

Funding: The Medical Research Council UK and Wellcome Trust funded MOSAIC via Programme Grant 090382/Z/09/Z, Imperial College London Comprehensive Biomedical Research Centre (cBRC) and Public Health England.

MOSAIC data and clinical samples were provided by the MOSAIC consortium*.

***The MOSAIC Investigators:**

Benaroya Research Institute, USA D. Chaussabel; **Gartnavel General Hospital, Greater Glasgow, UK** W. E. Adamson, W. F. Carman; **Health Protection Agency, UK** C. Thompson, M. C. Zambon; **Imperial College London, UK** P. Aylin, D. Ashby, W. S. Barclay, S. J. Brett, W. O. Cookson, L. N. Drumright, J. Dunning, R. A. Elderfield, L. Garcia-Alvarez, B. G. Gazzard, M. J. Griffiths, M. S. Habibi, T. T. Hansel, J. A. Herberg, A. H. Holmes, T. Hussell, S. L. Johnston, O. M. Kon, M. Levin, M. F. Moffatt, S. Nadel, P. J. Openshaw, J. O. Warner; **Liverpool School of Tropical Medicine, UK** S.J. Aston, S.B. Gordon; **National Institute for Medical Research, UK** A. Hay, J. McCauley, A. O'Garra; **Roche, Nutley, USA** J. Banchereau; **University College London, UK** A. Hayward; **University of**

Edinburgh, UK J. K. Baillie, D. A. Hume, P. Simmonds; **University of Liverpool, UK** P. S. McNamara, M. G. Semple, R. L. Smyth; **University of Nottingham, UK** J. S. Nguyen-Van-Tam; **University of Oxford, UK** L.-P. Ho, A. J. McMichael; **Wellcome Trust Sanger Institute, UK** P. Kellam. MOSAIC acknowledges the assistance of K. Alshafi, E. Bailey, A. Bermingham, M. Berry, C. Bloom, E. Brannigan, S. Bremang, J. Clark, M. C. Cox, M. Cross, L. A. Cumming, S. Dyas, J. England-Smith, J. Enstone, D. Ferreira, N. Goddard, A. Godlee, S. Gormley, M. Guiver, M. O. Hassan-Ibrahim, H. Hill, P. Holloway, K. Hoschler, G. Houghton, F. Hughes, R. R. Israel, A. Jepson, K. D. Jones, W. P. Kelleher, M. Kidd, K. Knox, A. Lackenby, G. Lloyd, H. Longworth, M. Minns, S. Mookerjee, S. Mt-Isa, D. Muir, A. Paras, V. Pascual, L. Rae, S. Rodenhurst, F. Rozakeas, E. Scott, E. Sergi, N. Shah, V. Sutton, J. Vernazza, A. W. Walker, C. Wenden, T. Wotherspoon, A. D. Wright, F. Wurie and the clinical and laboratory staff of the Alder Hey Children's NHS Foundation Trust; Brighton & Sussex University Hospitals NHS Trust, Central Manchester University Hospitals NHS Foundation Trust, Chelsea and Westminster Hospital NHS Foundation Trust, Alder Hey Children's Hospital and Liverpool School of Tropical Medicine; Health Protection Agency Microbiology Services Colindale; Imperial College Healthcare NHS Trust, Liverpool Women's NHS Foundation Trust, Royal Liverpool and Broadgreen University Hospitals NHS Trust, Royal Brompton and Harefield NHS Foundation Trust, The Roslin Institute, Edinburgh, University Hospitals Coventry and Warwickshire NHS Trust. The MOSAIC consortium was supported by several Comprehensive Local Research Networks (CLRNs), the National Institute for Health Research (NIHR), UK, and by the Biomedical Research Centre (BRC) and Unit (BRU) funds. Finally, we thank all patients and their relatives for their generous agreement to inclusion in this study.

660 **References**

661 1. **Zhou NN, Senne DA, Landgraf JS, Swenson SL, Erickson G, Rossow K,**
662 **Liu L, Yoon K j, Krauss S, Webster RG**. 1999. Genetic reassortment of
663 avian, swine, and human influenza A viruses in American pigs. J. Virol.
664 **73**:8851–8856.

665 2. **Karasin AI, Schutten MM, Cooper LA, Smith CB, Subbarao K, Anderson**
666 **GA, Carman S, Olsen CW**. 2000. Genetic characterization of H3N2 influenza
667 viruses isolated from pigs in North America, 1977-1999: Evidence for wholly
668 human and reassortant virus genotypes. Virus Res. **68**:71–85.

669 3. **Webby RJ, Swenson SL, Krauss SL, Gerrish PJ, Goyal SM, Webster RG**.
670 2000. Evolution of swine H3N2 influenza viruses in the United States. J. Virol.
671 **74**:8243–8251.

672 4. **Smith GJD, Vijaykrishna D, Bahl J, Lycett SJ, Worobey M, Pybus OG, Ma**
673 **SK, Cheung CL, Raghwani J, Bhatt S, Peiris JSM, Guan Y, Rambaut A**.
674 2009. Origins and evolutionary genomics of the 2009 swine-origin H1N1
675 influenza A epidemic. Nature **459**:1122–1125.

676 5. **Garten RJ, Davis CT, Russell C a, Shu B, Lindstrom S, Balish A, Sessions**
677 **WM, Xu X, Skepner E, Deyde V, Okomo-Adhiambo M, Gubareva L, Barnes**
678 **J, Smith CB, Emery SL, Hillman MJ, Rivailler P, Smagala J, de Graaf M,**
679 **Burke DF, Fouchier R a M, Pappas C, Alpuche-Aranda CM, López-Gatell**
680 **H, Olivera H, López I, Myers C a, Faix D, Blair PJ, Yu C, Keene KM,**
681 **Dotson PD, Boxrud D, Sambol AR, Abid SH, St George K, Bannerman T,**
682 **Moore AL, Stringer DJ, Blevins P, Demmler-Harrison GJ, Ginsberg M,**
683 **Kriner P, Waterman S, Smole S, Guevara HF, Belongia E a, Clark P a,**
684 **Beatrice ST, Donis R, Katz J, Finelli L, Bridges CB, Shaw M, Jernigan DB,**
685 **Uyeki TM, Smith DJ, Klimov AI, Cox NJ**. 2009. Antigenic and genetic
686 characteristics of swine-origin 2009 A(H1N1) influenza viruses circulating in
687 humans. Science **325**:197–201.

688 6. **Mänz B, Dornfeld D, Götz V, Zell R, Zimmermann P, Haller O, Kochs G,**
689 **Schwemmle M**. 2013. Pandemic Influenza A Viruses Escape from Restriction
690 by Human MxA through Adaptive Mutations in the Nucleoprotein. PLoS
691 Pathog. **9**.

692 7. **Hale BG, Steel J, Medina RA, Manicassamy B, Ye J, Hickman D, Hai R,**
693 **Schmolke M, Lowen AC, Perez DR, García-Sastre A**. 2010. Inefficient
694 control of host gene expression by the 2009 pandemic H1N1 influenza A virus
695 NS1 protein. J. Virol. **84**:6909–22.

696 8. **Shelton H, Smith M, Hartgroves LCS, Stilwell P, Roberts KL, Johnson B,**
697 **Barclay WS**. 2012. An influenza reassortant with polymerase of pH1N1 and
698 NS gene of H3N2 influenza A virus is attenuated in vivo. J. Gen. Virol. **93**:998–
699 1006.

9. **Sridhar S, Begom S, Bermingham A, Hoschler K, Adamson W, Carman W, Van Kerkhove MD, Lalvani A**. 2013. Incidence of influenza A(H1N1)pdm09 infection, United Kingdom, 2009-2011. Emerg. Infect. Dis. **19**:1866–9.

10. **Green HK, Andrews N, Fleming D, Zambon M, Pebody R**. 2013. Mortality Attributable to Influenza in England and Wales Prior to, during and after the 2009 Pandemic. PLoS One **8**:e79360.

11. **Presanis AM, Pebody RG, Paterson BJ, Tom BDM, Birrell PJ, Charlett A, Lipsitch M, De Angelis D**. 2011. Changes in severity of 2009 pandemic A/H1N1 influenza in England: a Bayesian evidence synthesis. BMJ **343**:d5408.

12. **Hayward AC, Fragaszy EB, Bermingham A, Wang L, Copas A, Edmunds WJ, Ferguson N, Goonetilleke N, Harvey G, Kovar J, Lim MSC, McMichael A, Millett ERC, Nguyen-Van-Tam JS, Nazareth I, Pebody R, Tabassum F, Watson JM, Wurie FB, Johnson AM, Zambon M**. 2014. Comparative community burden and severity of seasonal and pandemic influenza: results of the Flu Watch cohort study. Lancet Respir. Med.

13. **Mytton OT, Rutter PD, Donaldson LJ**. 2012. Influenza A (H1N1) pdm09 in England , 2009 to 2011 : a greater burden of severe illness in the year after the pandemic than in the pandemic year 1–9.

14. **Galiano M, Agapow P-M, Thompson C, Platt S, Underwood A, Ellis J, Myers R, Green J, Zambon M**. 2011. Evolutionary pathways of the pandemic influenza A (H1N1) 2009 in the UK. PLoS One **6**:e23779.

15. **Barr IG, Cui L, Komadina N, Lee RT, Lin RT, Deng Y, Caldwell N, Shaw R**. 2010. A new pandemic influenza A (H1N1) genetic variant predominated in the winter 2010 influenza season in Australia , New Zealand and Singapore. Euro Surveill. **15**:1–6.

16. **Dorigatti I, Cauchemez S, Ferguson NM**. 2013. Increased transmissibility explains the third wave of infection by the 2009 H1N1 pandemic virus in England. Proc. Natl. Acad. Sci. U. S. A. **110**:13422–7.

17. **Matrosovich M, Matrosovich T, Carr J, Roberts NA, Klenk H-D**. 2003. Overexpression of the alpha-2,6-sialyltransferase in MDCK cells increases influenza virus sensitivity to neuraminidase inhibitors. J. Virol. **77**:8418–25.

18. **Bao Y, Bolotov P, Dernovoy D, Kiryutin B, Zaslavsky L, Tatusova T, Ostell J, Lipman D**. 2008. The influenza virus resource at the National Center for Biotechnology Information. J. Virol. **82**:596–601.

19. **Tamura K, Stecher G, Peterson D, Filipski A, Kumar S**. 2013. MEGA6: Molecular Evolutionary Genetics Analysis version 6.0. Mol. Biol. Evol. **30**:2725–9.

20. **Baillie GJ, Galiano M, Agapow P-M, Myers R, Chiam R, Gall A, Palser AL, Watson SJ, Hedge J, Underwood A, Platt S, McLean E, Pebody RG, Rambaut A, Green J, Daniels R, Pybus OG, Kellam P, Zambon M**. 2012. Evolutionary dynamics of local pandemic H1N1/2009 influenza virus lineages revealed by whole-genome analysis. J. Virol. **86**:11–8.

21. **Watson SJ, Welkers MRA, Depledge DP, Coulter E, Breuer JM, de Jong MD, Kellam P**. 2013. Viral population analysis and minority-variant detection using short read next-generation sequencing. Philos. Trans. R. Soc. Lond. B. Biol. Sci. **368**:20120205.

22. **Van Doremalen N, Shelton H, Roberts KL, Jones IM, Pickles RJ, Thompson CI, Barclay WS**. 2011. A single amino acid in the HA of pH1N1 2009 influenza virus affects cell tropism in human airway epithelium, but not transmission in ferrets. PLoS One **6**:e25755.

23. **Hayman A, Comely S, Lackenby A, Hartgroves LCS, Goodbourn S, McCauley JW, Barclay WS**. 2007. NS1 proteins of avian influenza A viruses can act as antagonists of the human alpha/beta interferon response. J. Virol. **81**:2318–27.

24. **Thompson CI, Barclay WS, Zambon MC**. 2004. Changes in in vitro susceptibility of influenza A H3N2 viruses to a neuraminidase inhibitor drug during evolution in the human host. J. Antimicrob. Chemother. **53**:759–65.

25. **Blumenkrantz D, Roberts KL, Shelton H, Lycett S, Barclay WS**. 2013. The short stalk length of highly pathogenic avian influenza H5N1 virus neuraminidase limits transmission of pandemic H1N1 virus in ferrets. J. Virol. **87**:10539–51.

26. **Moncorgé O, Mura M, Barclay WS**. 2010. Evidence for avian and human host cell factors that affect the activity of influenza virus polymerase. J. Virol. **84**:9978–86.

27. **Ellis J, Galiano M, Pebody R, Lackenby A, Thompson C, Bermingham A, McLean E, Zhao H, Bolotin S, Dar O, Watson JM, Zambon M**. 2011. Virological analysis of fatal influenza cases in the United Kingdom during the early wave of influenza in winter 2010/11. Euro Surveill. **16**.

28. **Morlighem J-É, Aoki S, Kishima M, Hanami M, Ogawa C, Jalloh A, Takahashi Y, Kawai Y, Saga S, Hayashi E, Ban T, Izumi S, Wada A, Mano M, Fukunaga M, Kijima Y, Shiomi M, Inoue K, Hata T, Koretsune Y, Kudo K, Himeno Y, Hirai A, Takahashi K, Sakai-Tagawa Y, Iwatsuki-Horimoto K, Kawaoka Y, Hayashizaki Y, Ishikawa T**. 2011. Mutation analysis of 2009 pandemic influenza A(H1N1) viruses collected in Japan during the peak phase of the pandemic. PLoS One **6**:e18956.

29. **Falcone V, Bierbaum S, Kern W, Kontny U, Bertz H, Huzly D, Panning M**. 2013. Influenza virus A(H1N1)pdm09 hemagglutinin polymorphism and

associated disease in southern Germany during the 2010/11 influenza season. Arch. Virol. **158**:1297–303.

30. **Venter M, Naidoo D, Pretorius M, Buys A, McAnerney J, Blumberg L, Madhi SA, Cohen C, Schoub B**. 2012. Evolutionary dynamics of 2009 pandemic influenza A virus subtype H1N1 in South Africa during 2009-2010. J. Infect. Dis. **206 Suppl** :S166–72.

31. **Orelle A, Razanajatovo NH, Rajatonirina S, Hoffmann J, Randrianasolo L, Razafitrimo GM, Naidoo D, Richard V, Heraud J-M**. 2012. Epidemiological and virological characterization of 2009 pandemic influenza A virus subtype H1N1 in Madagascar. J. Infect. Dis. **206 Suppl** :S140–7.

32. **Chen G-W, Tsao K-C, Huang C-G, Gong Y-N, Chang S-C, Liu Y-C, Wu H-H, Yang S-L, Lin T-Y, Huang Y-C, Shih S-R**. 2012. Amino acids transitioning of 2009 H1N1pdm in Taiwan from 2009 to 2011. PLoS One **7**:e45946.

33. **Dapat IC, Dapat C, Baranovich T, Suzuki Y, Kondo H, Shobugawa Y, Saito R, Suzuki H**. 2012. Genetic characterization of human influenza viruses in the pandemic (2009-2010) and post-pandemic (2010-2011) periods in Japan. PLoS One **7**:e36455.

34. **Kao C-L, Chan T-C, Tsai C-H, Chu K-Y, Chuang S-F, Lee C-C, Li Z-RT, Wu K-W, Chang L-Y, Shen Y-H, Huang L-M, Lee P-I, Yang C, Compans R, Rouse BT, King C-C**. 2012. Emerged HA and NA mutants of the pandemic influenza H1N1 viruses with increasing epidemiological significance in Taipei and Kaohsiung, Taiwan, 2009-10. PLoS One **7**:e31162.

35. **Mir MA, Lal RB, Sullender W, Singh Y, Garten R, Krishnan A, Broor S**. 2012. Genetic diversity of HA1 domain of hemagglutinin gene of pandemic influenza H1N1pdm09 viruses in New Delhi, India. J. Med. Virol. **84**:386–93.

36. **Ledesma J, Pozo F, Reina G, Blasco M, Rodríguez G, Montes M, López-Miragaya I, Salvador C, Reina J, Ortíz de Lejarazu R, Egido P, López Barba J, Delgado C, Cuevas MT, Casas I**. 2012. Genetic diversity of influenza A(H1N1)2009 virus circulating during the season 2010-2011 in Spain. J. Clin. Virol. **53**:16–21.

37. **Lakspere T, Tynell J, Kaloinen M, Vanlede M, Parsons A, Ikonen N, Kallio-Kokko H, Kantele A, Mattila P, Almusa H, Julkunen I, Kainov D, Kakkola L**. 2014. Full-Genome Sequences of Influenza A(H1N1)pdm09 Viruses Isolated from Finnish Patients from 2009 to 2013. Genome Announc. **2**.

38. **Zhang Y, Zhang Q, Gao Y, He X, Kong H, Jiang Y, Guan Y, Xia X, Shu Y, Kawaoka Y, Bu Z, Chen H**. 2012. Key molecular factors in HA and PB2 contribute to the efficient transmission of the 2009 H1N1 pandemic influenza virus. J. Virol.

39. **Rodriguez A, Falcon A, Cuevas MT, Pozo F, Guerra S, García-Barreno B, Martinez-Orellana P, Pérez-Breña P, Montoya M, Melero JA, Pizarro M,**

Ortin J, Casas I, Nieto A. 2013. Characterization in vitro and in vivo of a pandemic H1N1 influenza virus from a fatal case. PLoS One **8**:e53515.

40. **Yang P, Deng J, Li C, Zhang P, Xing L, Li Z, Wang W, Zhao Y, Yan Y, Gu H, Liu X, Zhao Z, Zhang S, Wang X, Jiang C**. 2012. Characterization of the 2009 pandemic A/Beijing/501/2009 H1N1 influenza strain in human airway epithelial cells and ferrets. PLoS One **7**:e46184.

41. **Xu L, Bao L, Zhou J, Wang D, Deng W, Lv Q, Ma Y, Li F, Sun H, Zhan L, Zhu H, Ma C, Shu Y, Qin C**. 2011. Genomic polymorphism of the pandemic A (H1N1) influenza viruses correlates with viral replication, virulence, and pathogenicity in vitro and in vivo. PLoS One **6**:e20698.

42. **Yen H-L, Liang C-H, Wu C-Y, Forrest HL, Ferguson A, Choy K-T, Jones J, Wong DD-Y, Cheung PP-H, Hsu C-H, Li OT, Yuen KM, Chan RWY, Poon LLM, Chan MCW, Nicholls JM, Krauss S, Wong C-H, Guan Y, Webster RG, Webby RJ, Peiris M**. 2011. Hemagglutinin-neuraminidase balance confers respiratory-droplet transmissibility of the pandemic H1N1 influenza virus in ferrets. Proc. Natl. Acad. Sci. U. S. A. **108**:14264–9.

43. **Safronetz D, Rockx B, Feldmann F, Belisle SE, Palermo RE, Brining D, Gardner D, Proll SC, Marzi A, Tsuda Y, Lacasse RA, Kercher L, York A, Korth MJ, Long D, Rosenke R, Shupert WL, Aranda CA, Mattoon JS, Kobasa D, Kobinger G, Li Y, Taubenberger JK, Richt JA, Parnell M, Ebihara H, Kawaoka Y, Katze MG, Feldmann H**. 2011. Pandemic swine-origin H1N1 influenza A virus isolates show heterogeneous virulence in macaques. J. Virol. **85**:1214–23.

44. **Uraki R, Kiso M, Shinya K, Goto H, Takano R, Iwatsuki-Horimoto K, Takahashi K, Daniels RS, Hungnes O, Watanabe T, Kawaoka Y**. 2013. Virulence determinants of pandemic A(H1N1)2009 influenza virus in a mouse model. J. Virol. **87**:2226–33.

45. **Wedde M, Wählisch S, Wolff T, Schweiger B**. 2013. Predominance of HA-222D/G polymorphism in influenza A(H1N1)pdm09 viruses associated with fatal and severe outcomes recently circulating in Germany. PLoS One **8**:e57059.

46. **Zehender G, Pariani E, Piralla A, Lai A, Gabanelli E, Ranghiero A, Ebranati E, Amendola A, Campanini G, Rovida F, Ciccozzi M, Galli M, Baldanti F, Zanetti AR**. 2012. Reconstruction of the evolutionary dynamics of the A(H1N1)pdm09 influenza virus in Italy during the pandemic and post-pandemic phases. PLoS One **7**:e47517.

47. **Seyer R, Hrincius ER, Ritzel D, Abt M, Mellmann A, Marjuki H, Kühn J, Wolff T, Ludwig S, Ehrhardt C**. 2012. Synergistic Adaptive Mutations in the Hemagglutinin and Polymerase Acidic Protein Lead to Increased Virulence of Pandemic 2009 H1N1 Influenza A Virus in Mice. J. Infect. Dis. **205**:262–71.

48. **Zhang Y, Zhu J, Li Y, Bradley KC, Cao J, Chen H, Jin M, Zhou H**. 2013. Glycosylation on hemagglutinin affects the virulence and pathogenicity of pandemic H1N1/2009 influenza A virus in mice. PLoS One **8**:e61397.

49. **Strengell M, Ikonen N, Ziegler T, Julkunen I**. 2011. Minor changes in the hemagglutinin of influenza A(H1N1)2009 virus alter its antigenic properties. PLoS One **6**:e25848.

50. **De Vries RP, de Vries E, Martínez-Romero C, McBride R, van Kuppeveld F, Rottier PJM, García-Sastre A, Paulson JC, de Haan C a M**. 2013. Evolution of the hemagglutinin protein of new pandemic H1N1 virus: Maintaining optimal receptor binding by compensatory substitutions. J. Virol.

51. **Cotter CR, Jin H, Chen Z**. 2014. A single amino acid in the stalk region of the H1N1pdm influenza virus HA protein affects viral fusion, stability and infectivity. PLoS Pathog. **10**:e1003831.

52. **Takahashi T, Song J, Suzuki T, Kawaoka Y**. 2013. Mutations in NA that induced low pH-stability and enhanced the replication of pandemic (H1N1) 2009 influenza A virus at an early stage of the pandemic. PLoS One **8**:e64439.

53. **Meunier I, Embury-Hyatt C, Stebner S, Gray M, Bastien N, Li Y, Plummer F, Kobinger GP, von Messling V**. 2012. Virulence differences of closely related pandemic 2009 H1N1 isolates correlate with increased inflammatory responses in ferrets. Virology **422**:125–31.

54. **Zou W, Chen D, Xiong M, Zhu J, Lin X, Wang L, Zhang J, Chen L, Zhang H, Chen H, Chen M, Jin M**. 2013. Insights into the increasing virulence of the swine-origin pandemic H1N1/2009 influenza virus. Sci. Rep. **3**:1601.

55. **Farooqui A, Leon AJ, Lei Y, Wang P, Huang J, Tenorio R, Dong W, Rubino S, Lin J, Li G, Zhao Z, Kelvin DJ**. 2012. Heterogeneous virulence of pandemic 2009 influenza H1N1 virus in mice. Virol. J. **9**:104.

56. **Wang X, Zhou S, Chen Y, Wei M, Xiong W, Yi X, Jiang S, Pan C**. 2013. Multiple amino acid mutations in viral RNA polymerase may synergistically enhance the transmissibility and/or virulence of the 2009 pandemic influenza (H1N1) virus. Acta Virol. **57**:35–40.

57. **Sun Y, Xu Q, Shen Y, Liu L, Wei K, Sun H, Pu J, Chang K-C, Liu J**. 2014. Naturally occurring mutations in the PA gene are key contributors to increased virulence of pandemic H1N1/09 influenza virus in mice. J. Virol. **88**:4600–4.

58. **Pérez-González A, Rodriguez A, Huarte M, Salanueva IJ, Nieto A**. 2006. hCLE/CGI-99, a human protein that interacts with the influenza virus polymerase, is a mRNA transcription modulator. J. Mol. Biol. **362**:887–900.

59. **Huarte M, Sanz-Ezquerro JJ, Roncal F, Ortín J, Nieto A**. 2001. PA subunit from influenza virus polymerase complex interacts with a cellular protein with homology to a family of transcriptional activators. J. Virol. **75**:8597–604.

60. **Kawaguchi A, Nagata K**. 2007. De novo replication of the influenza virus RNA genome is regulated by DNA replicative helicase, MCM. EMBO J. **26**:4566–75.

61. **Bussey KA, Desmet EA, Mattiacio JL, Hamilton A, Bradel-Tretheway B, Bussey HE, Kim B, Dewhurst S, Takimoto T**. 2011. PA residues in the 2009 H1N1 pandemic influenza virus enhance avian influenza virus polymerase activity in mammalian cells. J. Virol. **85**:7020–8.

62. **Brookes DW, Miah S, Lackenby A, Hartgroves L, Barclay WS**. 2010. Pandemic H1N1 2009 influenza virus with the H275Y oseltamivir resistance neuraminidase mutation shows a small compromise in enzyme activity and viral fitness. J. Antimicrob. Chemother.

63. **Ramos I, Bernal-Rubio D, Durham N, Belicha-Villanueva A, Lowen AC, Steel J, Fernandez-Sesma A**. 2011. Effects of receptor binding specificity of avian influenza virus on the human innate immune response. J. Virol. **85**:4421–31.

64. **Twu KY, Noah DL, Rao P, Kuo R-L, Krug RM**. 2006. The CPSF30 binding site on the NS1A protein of influenza A virus is a potential antiviral target. J. Virol. **80**:3957–65.

65. **Kuo R-L, Krug RM**. 2009. Influenza a virus polymerase is an integral component of the CPSF30-NS1A protein complex in infected cells. J. Virol. **83**:1611–6.

66. **Everitt AR, Clare S, Pertel T, John SP, Wash RS, Smith SE, Chin CR, Feeley EM, Sims JS, Adams DJ, Wise HM, Kane L, Goulding D, Digard P, Anttila V, Baillie JK, Walsh TS, Hume DA, Palotie A, Xue Y, Colonna V, Tyler-Smith C, Dunning J, Gordon SB, Smyth RL, Openshaw PJ, Dougan G, Brass AL, Kellam P**. 2012. IFITM3 restricts the morbidity and mortality associated with influenza. Nature **484**:519–23.

67. **Zhang Y-H, Zhao Y, Li N, Peng Y-C, Giannoulatou E, Jin R-H, Yan H-P, Wu H, Liu J-H, Liu N, Wang D-Y, Shu Y-L, Ho L-P, Kellam P, McMichael A, Dong T**. 2013. Interferon-induced transmembrane protein-3 genetic variant rs12252-C is associated with severe influenza in Chinese individuals. Nat. Commun. **4**:1418.

68. **Wang Z, Zhang A, Wan Y, Liu X, Qiu C, Xi X, Ren Y, Wang J, Dong Y, Bao M, Li L, Zhou M, Yuan S, Sun J, Zhu Z, Chen L, Li Q, Zhang Z, Zhang X, Lu S, Doherty PC, Kedzierska K, Xu J**. 2014. Early hypercytokinemia is associated with interferon-induced transmembrane protein-3 dysfunction and predictive of fatal H7N9 infection. Proc. Natl. Acad. Sci. U. S. A. **111**:769–74.

935 **Figure Legends**

936 **Figure 1.** Phylogenetic relationship of complete influenza A(H1N1)pdm09 genomes.

937 The tree is rooted on A/California/04/2009, shown as a blue-filled circle. UK first-
938 wave isolates are highlighted as blue circles, while isolates sequenced by the
939 MOSAIC consortium are shown as red circles for second wave community and
940 hospitalised patients respectively, and green circles for third wave community and
941 hospitalised patients respectively. Isolates characterised in this study are indicated
942 with coloured arrows, while the inferred ancestral location of the asparagine-lysine
943 mutation in PA is indicated with a black arrow. Nodes with bootstrap support >75%
944 are highlighted with asterisks. The scale bar represents 0.002 substitutions/site.

945 **Figure 2.** Replication of A(H1N1)pdm09 viruses in cell culture.

946

947 Viral growth of 10 clinical isolates from first wave (blue), second wave (red), or third
948 wave (green) in a) MDCK cells and b) human nasal Mucilair™ cell cultures (HAE)
949 (Epithelix). Cells were infected at an MOI of 0.001 (MDCK cells) 0.01 (Mucilair™)
950 and incubated at 34oC, the dashed line represents the mean of A/195.Statistics in
951 the tables adjoining the chart keys were calculated using unpaired t-tests with Holm-
952 Sidak corrections.

953 c) Replication of a representative first wave (A/195, blue circles) and third wave
954 (A/687, green squares) virus pair were assessed in HAE cells, (left panel) MDCK
955 cells (left middle panel), CALU3 cells (right middlepanel) and pig tracheal cells

(NPTr) (right panel). Cells were infected at MOI of 0.001. Statistics were calculated using unpaired t-tests.

Figure 3. Infection of mice with A(H1N1)pdm09 viruses

Weight loss following infection of fifteen Balb/C mice inoculated intranasally with 2 x105 PFU of virus isolates , a) one A/195 first wave isolate (blue), b) three 2nd wave isolates (red) and c) six 3rd wave isolates (green). Weight in mice inoculated with PBS is shown in black. Virus titre (d) and interferon levels (e) in lung homogenate at day 2. (f) Mouse mortality data for virus infections where weight loss necessitated cull.

Figure 4. Cytokine induction by first and third wave virus and the role of NS gene segment in virus replication in HAE.

a) Human nasal Mucilair™ cell cultures (HAE) (Epithelix) were infected in triplicate with RG A/195 and A/687 virus at MOI of 1 for 16 hours. The basal media was harvested and levels of the cytokine IP-10 measured using mesoscale discovery (MSD) plates. Stats: Unpaired t-test.

b) 293T cells transiently transfected with an interferon b promoter luciferase reporter plasmid were infected with RG viruses A/195 (dark blue), A/195 with A/687 segment 8 (light green), A/687 (dark green) and A/687 with the A/195 segment 8 (light blue) at an MOI of 3. Infection with Newcastle Disease Virus NDV was used as positive control. Stats: one way anova, with Turkey's multiple comparison test (and associated adjusted p values).

977 c) 293T cells transiently transfected with an interferon b promoter luciferase reporter
978 and pCAGGs NS1 plasmids A/195 (blue), A/687 (green) and H3N2 (purple).
979 Stimulated with NDV. Stats: one way anova with Turkey's multiple comparison test.

980 **Figure 5.** Variation in surface genes HA and NA in third wave virus leads to altered
981 receptor binding, enhanced replication in HAE cells and enhanced infectivity in
982 mucus.

983 a) Haemagglutination assay with 11 clinical isolates from first wave (blue), second
984 wave (red) and third wave (green) assessed for binding to 0.5% chicken, turkey or
985 guinea pig red blood cells, the dashed line represents the A195 HA score. . b)
986 Haemagglutination assay with equal PFU of A/195 first wave (blue) and A/687 third
987 wave (green) RG viruses with 0.5% chicken or turkey red blood cells. c) Viral
988 replication in human nasal Mucilair™ cell cultures (HAE) (Epithelix) of RG viruses
989 based on A/195 with HA and NA from A/195 first wave (blue) or HA and NA of
990 A/687 third wave (green triangle) d) A/687 (green square) or A/687 with A/687 with
991 HA and NA from A/195 (blue triangle)-. Cells were infected at an MOI of 0.01.* $p <$
992 0.05 by unpaired t test.

993 e) Mucus inhibition assay. An equal PFU of A/195 (blue) or A/195 with A/687 third
994 wave NA (green) RG virus was incubated with diluted human mucus for one hour
995 prior to infection on MDCK cells. Infectivity remaining was plotted as a percentage of
996 titre in absence of mucus. * p,0.044 by unpaired t test.

997 **Figure 6**. PA of third wave virus confers enhanced polymerase activity and a fitness
998 advantage in HAE cells.

a) Activity of polymerase reconstituted from plasmids expressing polymerase components of A/195 first wave (dark blue) and A/687 third wave (dark green) virus. 293T cells were transiently transfected with a plasmid that directs *in situ* synthesis of a minigenome in which a luciferase reporter gene is flanked by the influenza A promoter. Co-transfection of a Renilla expression plasmid was used to normalize for transfection efficiency. Combinations of the PB1, PB2, PA and NP expression plasmids of A/195 (blue) or A/687 (green) or lacking the PB2 polymerase (white) were transfected. 24 hours post transfection cells were harvested. The results were normalised to Renilla (transfection control) and are from three separate set of experiments each with triplicate wells (n=9). Differences were analysed using one-way Anova test with Tukey's multiple comparison test.

b) Human nasal Mucilair™ cell cultures (HAE) (Epithelix) were infected in triplicate with RG viruses based on A/195 that differed only in PA at N321K. Virus released was harvested at 24, 48, 72 & 96 hours and Illumina sequenced. The percentage of N allele (first wave) is represented in blue and K (third wave) in green.

1015 **Table 1)** Amino acid changes observed in 10 A/H1N1 pdm(2009) viruses isolated in
1016 the UK compared to prototypic virus A/England/195/2009. The three isolates from
1017 the 2009-2010 season are above the line and the 6 isolates from 2010-2011 are
1018 below.

1019 **Table 2)** Prevalence ratios of amino acid changes in the UK and the rest of the
1020 World (RoW) during the 1st, 2nd and 3rd waves of virus infection. Incomplete ratios are
1021 due to unknown or multiple minor populations. HA numbering is H1.

1022

1023 **Table 3)** Patient information for the MOSAIC viral isolates.

1024 Severity score was assigned according to severity of respiratory impairment: grade 1
1025 = no respiratory compromise (oxygen saturation >93% on room air); grade 2 =
1026 respiratory compromise requiring non-invasive oxygen supplementation; grade 3 =
1027 respiratory compromise requiring invasive mechanical ventilation and oxygen
1028 supplementation. Predisposing (co-morbid) conditions included asthma,
1029 immunosuppression etc. Collection month of sample the virus was isolated from and
1030 sample types in which virus was detected (NPA – nasopharyngeal aspirate; nk: not
1031 known). The time lag between onset of symptom and the viral sample is noted. Viral
1032 titre was assessed by qPCR of the H1N1 NA gene and run against a standard curve
1033 of viral RNA of know PFU/ML.

1034

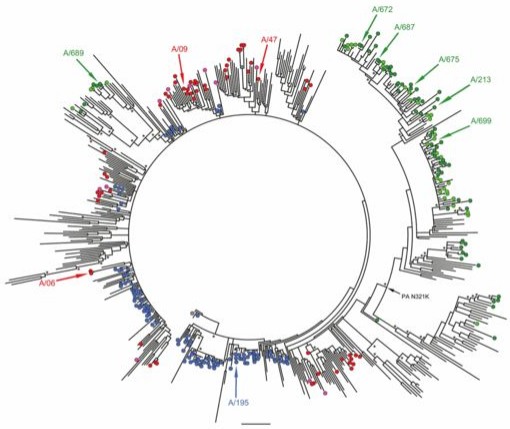

Figure 1. Phylogenetic relationship of complete influenza A(H1N1)pdm09 genomes.
The tree is rooted on A/California/04/2009, shown as a blue-filled circle. UK first-wave isolates are highlighted as blue circles, while isolates sequenced by the MOSAIC consortium are shown as red circles for second wave community and hospitalised patients respectively, and green circles for third wave community and hospitalised patients respectively. Isolates characterised in this study are indicated with coloured arrows, while the inferred ancestral location of the asparagine-lysine mutation in PA is indicated with a black arrow. Nodes with bootstrap support >75% are highlighted with asterisks. The scale bar represents 0.002 substitutions/site.

Figure 2

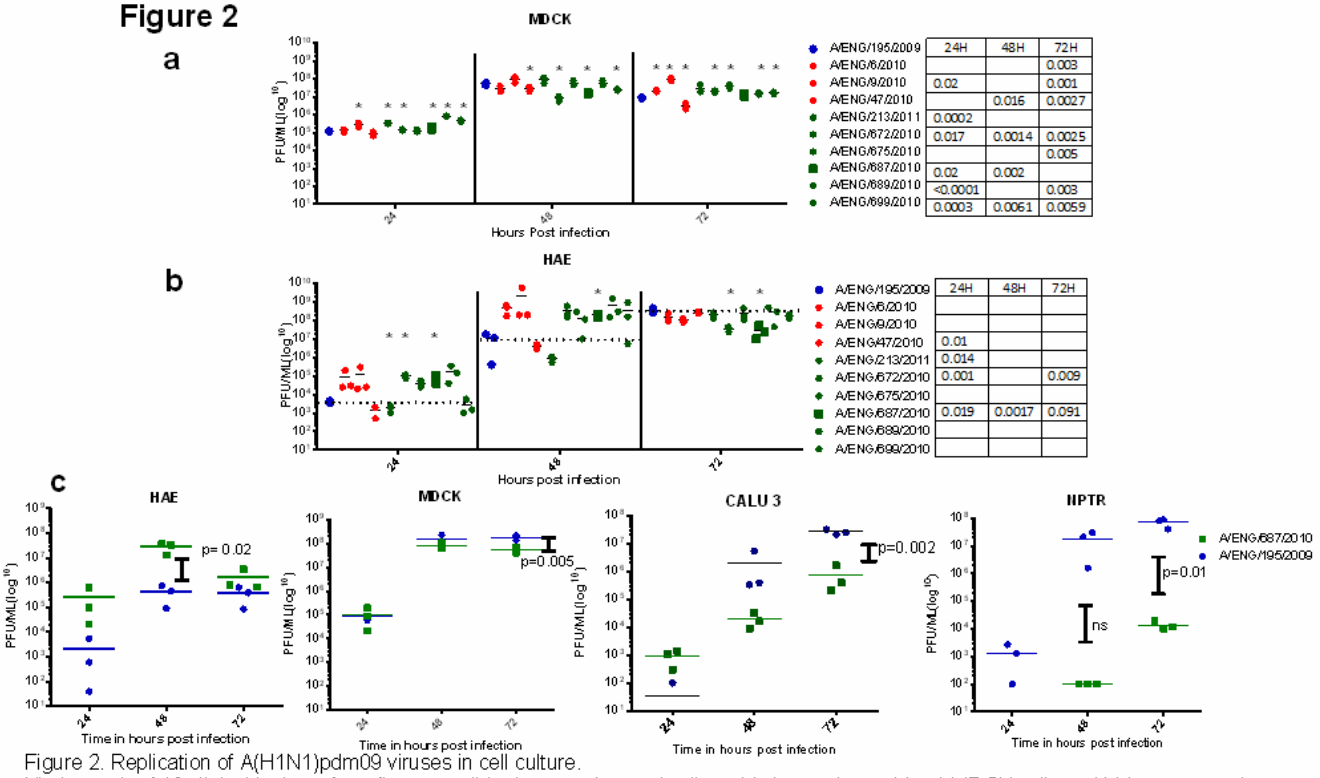

Figure 2. Replication of A(H1N1)pdm09 viruses in cell culture.
Viral growth of 10 clinical isolates from first wave (blue), second wave (red), or third wave (green) in a) MDCK cells and b) human nasal Mucilair™ cell cultures (HAE) (Epithelix). Cells were infected at an MOI of 0.001 (MDCK cells) 0.01 (Mucilair™) and incubated at 34oC, the dashed line represents the mean of A/195.Statistics in the tables adjoining the chart keys were calculated using unpaired t-tests with Holm-Sidak corrections.
c) Replication of a representative first wave (A/195, blue circles) and third wave (A/687, green squares) virus pair were assessed in HAE cells, (left panel) MDCK cells (left middle panel), CALU3 cells (right middlepanel) and pig tracheal cells (NPTr) (right panel). Cells were infected at MOI of 0.001. Statistics were calculated using unpaired t-tests.

Figure 3

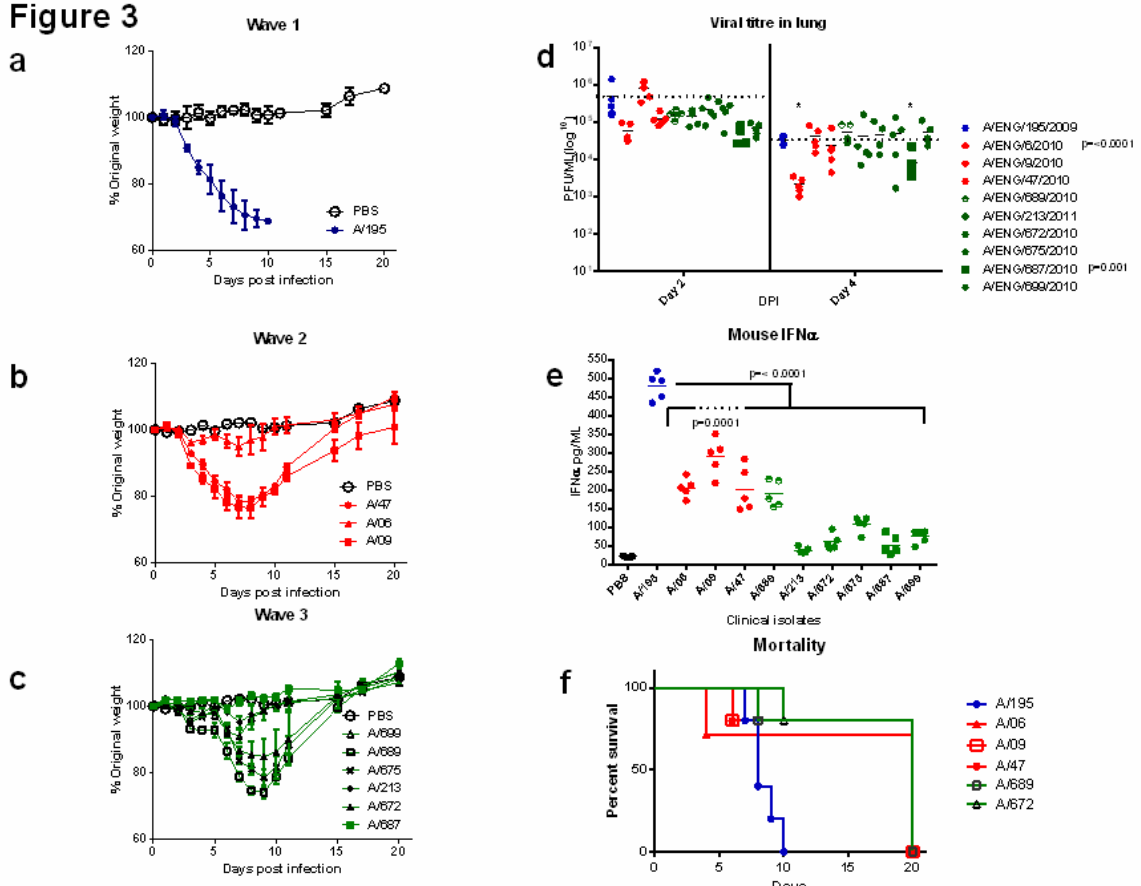

Figure 3. Infection of mice with A(H1N1)pdm09 viruses

Weight loss following infection of fifteen Balb/C mice inoculated intranasally with 2 x105 PFU of virus isolates , a) one A/195 first wave isolate (blue), b) three 2nd wave isolates (red) and c) six 3rd wave isolates (green). Weight in mice inoculated with PBS is shown in black. Virus titre (d) and interferon levels (e) in lung homogenate at day 2. (f) Mouse mortality data for virus infections causing weight loss necessitated cull.

Figure 4

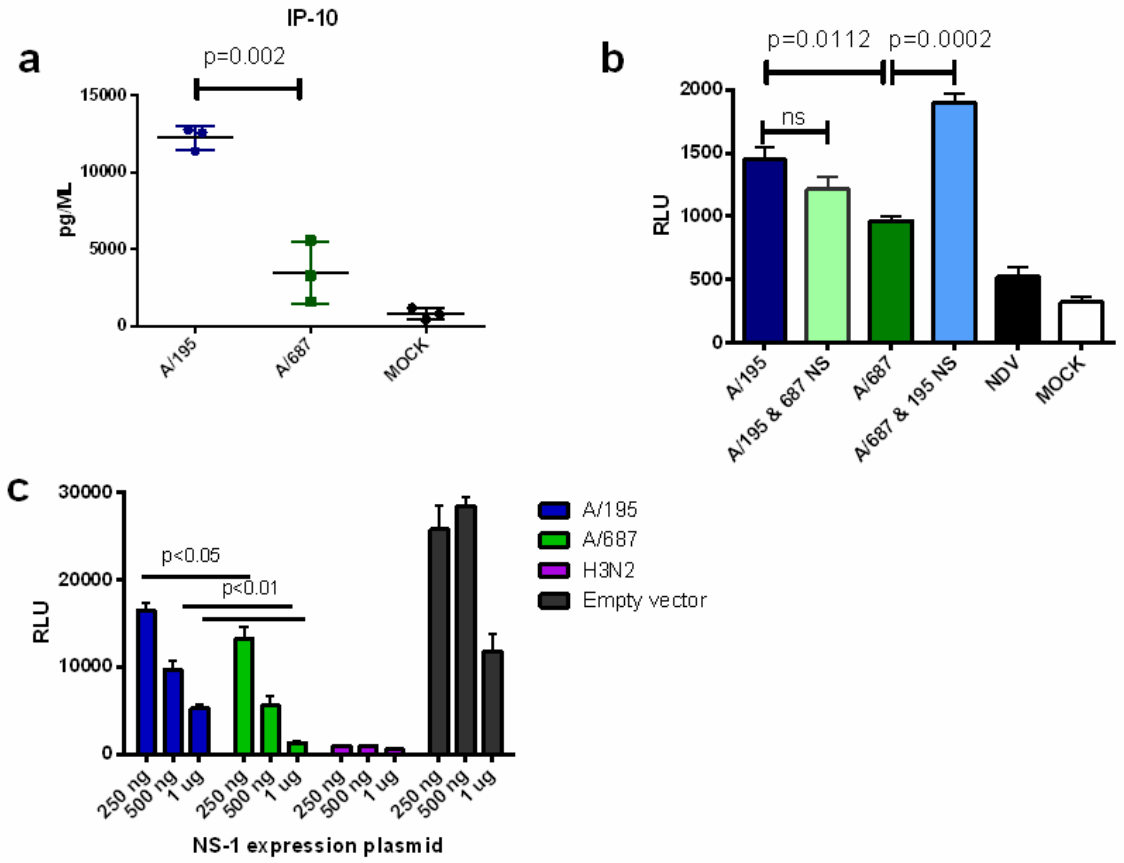

Figure 4. Cytokine induction by first and third wave virus and the role of NS gene segment in virus replication in HAE.

a) Human nasal Mucilair™ cell cultures (HAE) (Epithelix) were infected in triplicate with RG A/195 and A/687 virus at MOI of 1 for 16 hours. The basal media was harvested and levels of the cytokine IP -10 measured using mesoscale discovery (MSD) plates. Stats: Unpaired t-test.
b) 293T cells transiently transfected with an interferon b promoter luciferase reporter plasmid were infected with RG viruses A/195 (dark blue), A/195 with A/687 segment 8 (light green), A/687 (dark green) and A/687 with the A/195 segment 8 (light blue) at an MOI of 3. Infection with Newcastle Disease Virus NDV was used as positive control. Stats: one way anova, with Turkey's multiple comparison test (and associated adjusted p values).
c) 293T cells transiently transfected with an interferon b promoter luciferase reporter and pCAGGs NS1 plasmids A/195 (blue), A/687 (green) and H3N2 (purple). Stimulated with ND V. Stats: one way anova with Turkey's multiple comparison test.

Figure 5

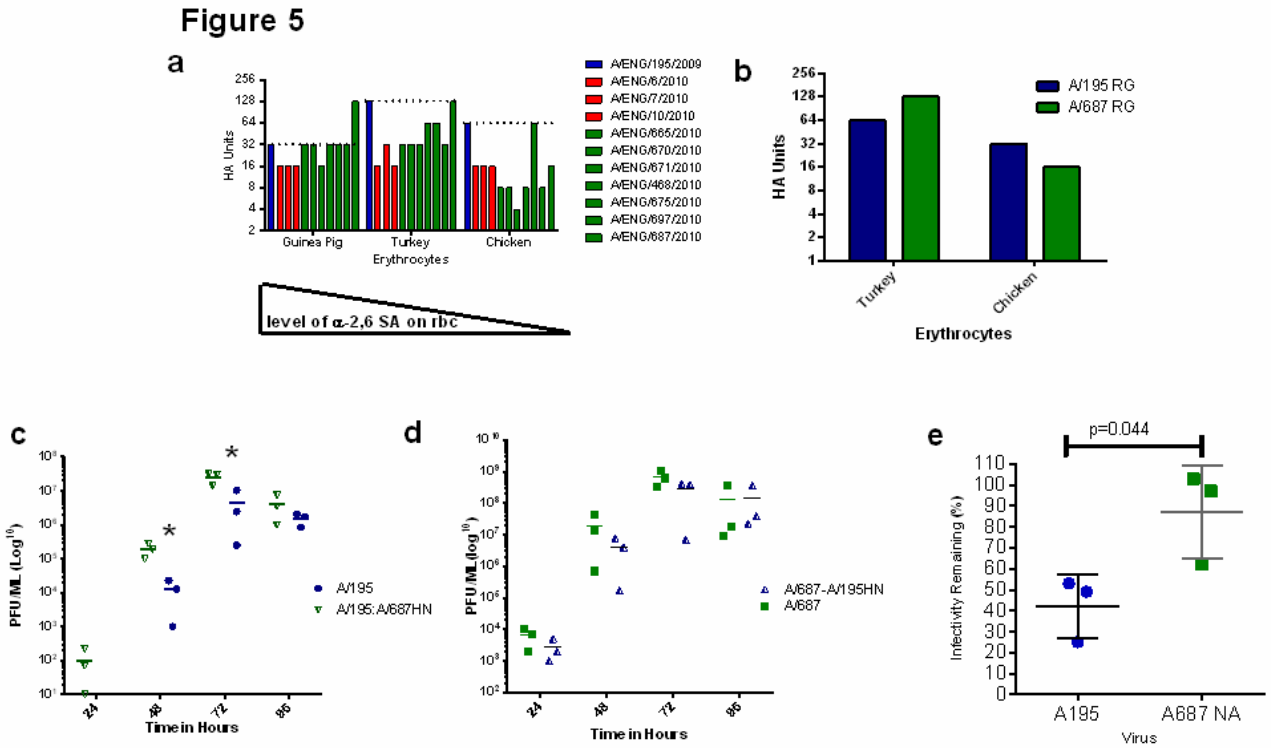

Figure 5. Variation in surface genes HA and NA in third wave virus leads to altered receptor binding, enhanced replication in HAE cells and enhanced infectivity in mucus.

a) Haemagglutination assay with 11 clinical isolates from first wave (blue), second wave (red) and third wave (green) assessed for binding to 0.5% chicken, turkey or guinea pig red blood cells, the dashed line represents the A195 HA score. . b) Haemagglutination assay with equal PFU of A/195 first wave (blue) and A/687 third wave (green) RG viruses with 0.5% chicken or turkey red blood cells. c) Viral replication in human nasal Mucilair™ cell cultures (HAE) (Epithelix) of RG viruses based on A/195 with HA and NA from A/195 first wave (blue) or HA and NA of A/687 third wave (green triangle) d) A/687 (green square) or A/687 with A/687 with HA and NA from A/195 (blue triangle)-. Cells were infected at an MOI of 0.01.* $p < 0.05$ by unpaired t test.

e) Mucus inhibition assay. An equal PFU of A/195 (blue) or A/195 with A/687 third wave NA (green) RG virus was incubated with diluted human mucus for one hour prior to infection on MDCK cells. Infectivity remaining was plotted as a percentage of titre in absence of mucus. * p,0.044 by unpaired t test.

Figure 6

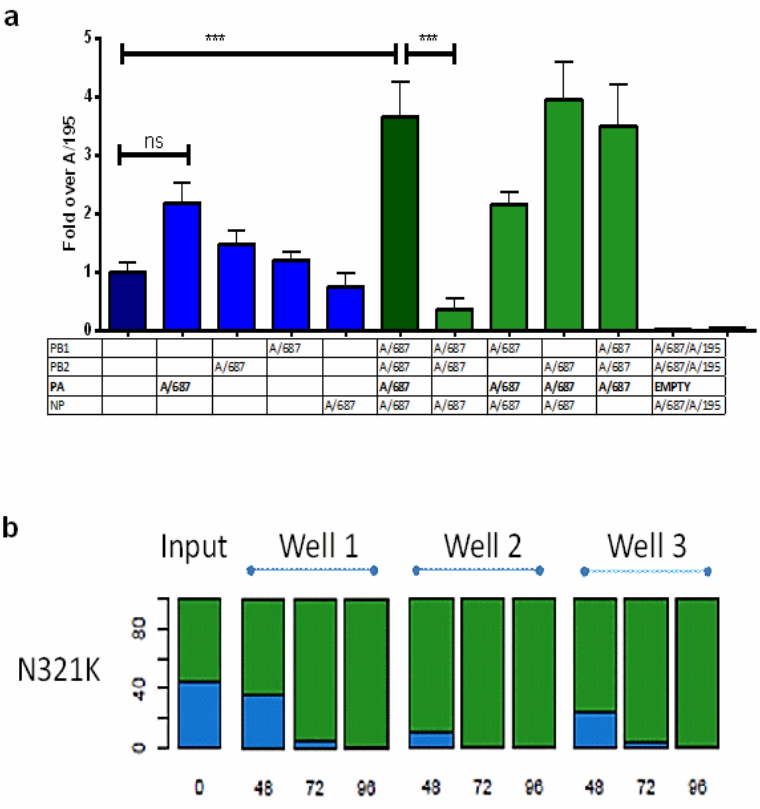

Figure 6. PA of third wave virus confers enhanced polymerase activity and a fitness advantage in HAE cells.

a) Activity of polymerase reconstituted from plasmids expressing polymerase components of A/195 first wave (dark blue) and A/687 third wave (dark green) virus. 293T cells were transiently transfected with a plasmid that directs in situ synthesis of a minigenome in which a luciferase reporter gene is flanked by the influenza A promoter. Co-transfection of a Renilla expression plasmid was used to normalize for transfection efficiency. Combinations of the PB1, PB2, PA and NP expression plasmids of A/195 (blue) or A/687 (green) or lacking the PB2 polymerase (white) were transfected. Twenty four hours post transfection cells were harvested with passive lysis bufffer (Promega), freeze:thawed and subjected to a luciferase assay. The results were normalised to Renilla (transfection control) and are from three separate set of experiments each with triplicate wells (n=9). Differences were analysed using one-way Anova test with Tukey's multiple comparison test.

b) Human nasal Mucilair™ cell cultures (HAE) (Epithelix) were infected in triplicate with RG viruses based on A/195 that differed only in PA at N321K. Virus released was harvested at 24, 48, 72 & 96 hours by incubation of the apical layer in serum free DMEM for 30 min. The apical supernatant was then removed and stored at 80oC prior to viral RNA extraction and Illumina sequencing. The percentage of N allele (first wave) is represented in blue and K (third wave) in green.

Table 1

	PB1							PB2															
	12	211	353	386	645	652	719	90	191	214	221	255	299	344	354	373	463	511	556	584	588	654	677
A/ENG/195/2009	I	R	R	K	V	A	V	M	E	K	A	V	R	V	I	R	I	V	N	V	T	P	G
A/ENG/06/2010			K			V	M										V						E
A/ENG/09/2010			K						K		S												E
A/ENG/47/2010			K	R												K							E
A/ENG/213/2011			K											M	L					I		Q	E
A/ENG/672/2010	T		K											M	L				S				E
A/ENG/675/2010			K											M	L								E
A/ENG/687/2010			K											M	L								E
A/ENG/689/2010		K	K			V		V		R		I						I			I		E
A/ENG/699/2010			K		I								K	M	L				S		A		E

	PA											NP	
	3	14	184	261	294	321	330	407	479	644	716	23	100
A/ENG/195/2009	G	V	S	L	D	N	I	V	D	S	K	T	V
A/ENG/06/2010	D										E	S	I
A/ENG/09/2010	D	I								Y			I
A/ENG/47/2010	D								E				I
A/ENG/213/2011	D		N		N	K							I
A/ENG/672/2010	D					K							I
A/ENG/675/2010	D			F		K							I
A/ENG/687/2010	D					K							I
A/ENG/689/2010	D							I	E				I
A/ENG/699/2010	D					K	V						I

	NA										M1		M2	NS1					NEP
	45	46	106	155	188	241	248	249	369	394	80	133	13	55	114	123	125	189	32
A/ENG/195/2009	Q	I	V	Y	I	V	N	G	N	V	V	N	S	E	P	I	E	G	V
A/ENG/06/2010			I				D									A	G		
A/ENG/09/2010			I				D									V			
A/ENG/47/2010			I				D	R								V			
A/ENG/213/2011			I	H	T	I	D		K		I				T	V			
A/ENG/672/2010			I			I	D		K		I				T			D	I
A/ENG/675/2010	K	T	I			I	D		K		I		N		T	V			
A/ENG/687/2010			I			I	D		K		I				T	V		D	I
A/ENG/689/2010			I				D			I		S		Q		V			
A/ENG/699/2010			I			I	D		K		I					V			

	HA																		
H1	32	56	96	97	134	168	176	183	185	203	205	227	370	374	404	441	451	499	510
1'Met	49	73	113	114	151	185	193	200	202	220	222	244	387	391	421	458	468	516	527
A/ENG/195/2009	I	N	I	D	A	D	L	S	S	S	R	M	N	E	I	N	S	E	I
A/ENG/06/2010	L		T							T									
A/ENG/09/2010	L	D								T			H		V				V
A/ENG/47/2010										T								K	
A/ENG/213/2011	L			N		N			T	T				K			N		
A/ENG/672/2010	L	S		N					T	T				K			N		
A/ENG/675/2010	L			N					T	T	K	I		K			N		
A/ENG/687/2010	L	S		N			I		T	T				K			N		
A/ENG/689/2010	L				T			P		T						K			
A/ENG/699/2010	L			N					T	T				K			N		

Table 1. Amino acid changes observed in 10 A/H1N1 pdm(2009) viruses isolated in the UK compared to prototypic virus A/England/195/2009. The three isolates from the 2009-2010 season are above the line and the 6 isolates from 2010-2011 are below.

PB1	R353K	
	K	R
UK 1st	82	17
RoW 1st	89	10
UK 2nd	100	
RoW 2nd	98	2
UK 3rd	98	1
RoW 3rd	97	1

HA	I32L		D97N		S185T		S203T		E374K		S451N	
	L	I	D	N	S	T	T	S	E	K	S	N
UK 1st	87	13	98		98		62	38	99	1	100	
RoW 1st	94	6	99	1	99		63	37	97	2	99	1
UK 2nd	94	6	95	2	100		98	2	68	31	97	3
RoW 2nd	96	4	94	6	99		94	5	68	30	99	1
UK 3rd	100		27	73	16	82	99	1	11	86	15	84
RoW 3rd	100		44	56	16	83	100		6	94	16	84

PB2	V344M		I354L		G677E	
	V	M	I	L	E	G
UK 1st	100		100		97	3
RoW 1st	99	1	100		99	1
UK 2nd	100		100		100	
RoW 2nd	97	2	99		99	1
UK 3rd	12	87	12	86	99	
RoW 3rd	18	81	19	81	100	

NA	V106I		V241I		N248D		N369K	
	I	V	V	I	D	N	N	K
UK 1st	58	42	99	1	57	42	100	
RoW 1st	77	23	98		77	23	100	
UK 2nd	99	1	99	1	99		100	
RoW 2nd	97	3	99		98	2	98	1
UK 3rd	98	1	12	87	99	1	13	85
RoW 3rd	76	24	14	85	99	1	15	85

PA	G3D		N321K	
	D	G	N	K
UK 1st	88	12	100	
RoW 1st	98	2	99	
UK 2nd	99		99	
RoW 2nd	99		99	
UK 3rd	99		15	84
RoW 3rd	100		21	78

M1	V80I	
	V	I
UK 1st	100	
RoW 1st	100	
UK 2nd	100	
RoW 2nd	100	
UK 3rd	17	82
RoW 3rd	20	80

NP	V100I	
	I	V
UK 1st	55	45
RoW 1st	78	22
UK 2nd	96	4
RoW 2nd	97	3
UK 3rd	99	1
RoW 3rd	98	2

NS1	P114T		I123V/A			G189D		NEP	V32I	
	P	T	I	V	A	G	D		V	I
UK 1st	100		54	46		100			100	
RoW 1st	100		42	58		100			100	
UK 2nd	100		4	95	2	100			100	
RoW 2nd	99		6	94		99	1		99	1
UK 3rd	61	39	2	96	2	85	15		85	15
RoW 3rd	93	5	1	98	1	99	1		99	1

Table 2) Prevalence ratios of amino acid changes in the UK and the rest of the World (RoW) during the 1st, 2nd and 3rd waves of virus infection. Incomplete ratios are due to unknown or multiple minor populations. HA numbering is H1.

Isolate	Severity Score	Co-morbidities	Collection date	Day since symptom onset	Viral detection	T1 NPA Titre (PFU/ML)
A/England/195/2009	mild*	nk	Apr-09	Nk	nk	Nk
A/England/06/2010	1	Yes	Jan-10	20	NPA	5802
A/England/09/2010	1	Yes	Dec-09	2	NPA	7035
A/England/47/2010	3	Yes	Dec-09	9	NPA, Blood, Stool	2315
A/England/213/2011	2	Yes	Jan-11	1	NPA	47
A/England/672/2010	2	Yes	Dec-10	4	NPA	0.2
A/England/675/2010	1	No	Dec-10	2	NPA	2
A/England/687/2010	2	Yes	Dec-10	2	NPA	8
A/England/689/2010	1	Yes	Dec-10	2	NPA	1251
A/England/699/2010	3	Yes	Dec-10	4	NPA	23

Table 3) Patient information for the MOSAIC viral isolates. Severity score was assigned according to severity of respiratory impairment: grade 1 = no respiratory compromise (oxygen saturation >93% on room air); grade 2 = respiratory compromise requiring non-invasive oxygen supplementation; grade 3 = respiratory compromise requiring invasive mechanical ventilation and oxygen supplementation.. Predisposing (co-morbid) conditions included asthma, immunosuppression etc. Collection month of sample the virus was isolated from and sample types in which virus was detected (NPA - nasopharyngeal aspirate; nk: not known). The time lag between onset of symptom and the viral sample is noted. Viral titre was assessed by qPCR of the H1N1 NA gene and run against a standard curve of viral RNA of know PFU/ML.